SUPERVISED MORPHOLOGICAL TARGET DETECTION FROM POLARIMETRIC STOKES VECTORS IMAGES

Joana Frontera-Pons[1], Jesus Angulo[2]

[1]SONDRA Research Alliance, Supélec, France
[2] CMM-Centre de Morphologie Mathématique, Mathématiques et Systèmes, MINES Paristech, France

ABSTRACT

This papers deals with supervised ordering on the unit hypersphere, which yields a rich framework for the generalization of all morphological operators on the sphere. In particular, supervised openings/closings and supervised hit-or-miss are introduced. Various strategies on the computation of the supervised ordering are considered and the different alternatives are studied for the purpose of structured target detection.

Index Terms— mathematical morphology, polarimetric image processing, supervised ordering

1. INTRODUCTION

Fully polarimetric synthetic aperture radar (PolSAR) provides data containing the complete scattering information. Therefore, these data have drawn more attention in recent years. PolSAR data can be represented as polarization states on a sphere. We present image processing techniques based on the analysis of the polarimetric information within its location on the sphere.

Mathematical morphology is a well-known nonlinear approach for image processing. It is based on the computation of minimum and maximum values of local neighborhoods. That necessitates the existence of an ordering relationship between the points to be treated. The lack of a natural ordering on the sphere presents an inherent problem when defining morphological operators extended to unit sphere. We analyze here some proposals to the problem of ordering on the unit sphere, leading to formulations of morphological operators suited to the configuration of the data. Supervised orderings are considered and its associated operators for target recognition issues. The aim is to detect structured targets of size larger than one pixel. The different methods may ultimately provide useful tools when searching specific types of targets in heterogeneous clutter. The key assumption is that a training set for the target and for each of the different components of the background are available.

2. POLARIMETRIC STATE ON THE SPHERE

The Stokes vector. Polarization refers to the alignment and the regularity of the Electric and Magnetic fields in the plane perpendicular to the propagation direction. The Electric field is described as the sum of two orthogonal components (horizontal and vertical) with different amplitude and a relative phase between them. Therefore, the tip of Electric field vector of a totally polarized wave depicts a regular pattern, in general cases elliptical. The polarization ellipse can be completely characterized by its orientation ψ and the shape parameter χ called ellipticity. Hence the polarization state may be represented by ψ, χ and a parameter S_0 proportional to the total wave intensity, and it can be written in vector form according to the Stokes vector:

$$\begin{bmatrix} S_0 \\ S_1 \\ S_2 \\ S_3 \end{bmatrix} = \begin{bmatrix} |E_v|^2 + |E_h|^2 \\ |E_v|^2 - |E_h|^2 \\ 2\Re\{E_v E_h^*\} \\ 2\Im\{E_v E_h^*\} \end{bmatrix} = \begin{bmatrix} S_0 \\ S_0 \cos 2\psi \cos 2\chi \\ S_0 \sin 2\psi \cos 2\chi \\ S_0 \sin 2\chi \end{bmatrix}$$
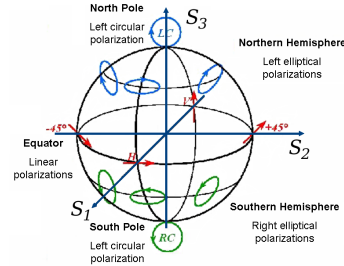
Polarization state on the sphere $\mathbb{S}^2$**.** For a completely polarized wave, the polarization state can be described by a point on the Poincaré sphere, noted by $\xi_i \in \mathbb{S}^2$. The radius of the sphere is S_0, the intensity of the wave. The latitude of the point corresponds to 2χ and the longitude to 2ψ. Then the linear polarizations lie on the equator, with horizontal and vertical polarizations opposite each other. Moreover, left-hand circular and right-hand circular polarizations are placed on the north and south poles respectively. All other points represent elliptical polarization with certain χ and ψ. Opposite points on the sphere, antipodal points, represent polarizations that are orthogonal to one another and are called cross-polarizations. To place the polarization on the sphere, we represent the last three Stokes parameters as components in a three-dimensional vector space. Fig. 1 provides a typical example of polarimetric simulated image which has been used in this paper.

(a) $f(x,y) : \mathbb{Z}^2 \to \mathbb{S}^2$ (b) $\mathbb{S}^2$
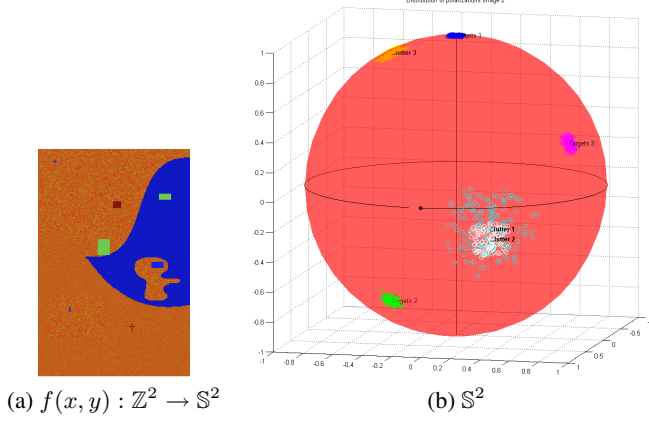
Fig. 1. (a) Image valued on $\mathbb{S}^2$ that exemplifies a complex scenario with three types of targets of different sizes and three clutters. (b) Image values on the sphere showing the dispersion (noise) for each object.

3. $H-$SUPERVISED ORDERING ON $\mathbb{S}^2$

For nonlinear image processing on the sphere $\mathbb{S}^2$, it is necessary to define a bijective mapping h that establishes a complete lattice structure on set $\mathcal{L}$, i.e., $h : \mathbb{S}^2 \to \mathcal{L}$ where, typically, $\mathcal{L}$ can be identified as the real values set. Once an ordering is determined for a set $R \subset \mathbb{S}^2$, morphological processing can be directly performed. The notion of *h-supervised ordering* was recently introduced in [8]. Let us particularize this approach to the case of $\mathbb{S}^2$ in the context of radar polarimetric imaging, which involves the notions of target and clutter. From a nonempty set S of values on $\mathbb{S}^2$ (the training set), which is composed of the subsets T and C, such that $S = T \cup C$ and $T \cap C = \emptyset$, a *h-supervised ordering from S* satisfies the conditions: $h(t) = \top$ if $t \in T$, and $h(c) = \bot$ if $c \in C$. where $\top$ denotes the maximum element in $\mathcal{L}$, whilst $\bot$ refers to the minimum element of $\mathcal{L}$. Therefore, taking into account the information contained in the data, we identify: T as the *target training set* $T \equiv \mathcal{V}_\top = \{t_i\}_{i=1}^I$, which is related to the distribution of values of the image structures we intend to detect; and C as the *clutter training set* $C \equiv \mathcal{V}_\bot = \{c_j\}_{j=1}^J$, which sorts the corresponding background of the scenario to analyze.

Now, for any subset of values $R = \{\xi_k\}_{k=1}^N$, $\xi_k \in \mathbb{S}^2$ we define the supervised ordering mapping

$$h(\xi_k) = K(\xi_k, T) - K(\xi_k, C) \qquad (1)$$

where the kernel $K(\cdot, \cdot) : \mathbb{S}^2 \times \{\mathbb{S}^2\} \to \mathbb{R}^+$ is a function based on distances between a point ξ_k and a set of points (training sets target or clutter). We notice that in that case $h : \mathbb{S}^2 \to \mathbb{R}$. A first single way consists in characterizing sets of training T and C by their first order statistics μ° (average on the sphere, we have considered the Fréchet-Karcher barycenter, detailed in [1, 2]): $t = \mu^\circ(T)$ and $c = \mu^\circ(T)$.

Then, an useful value of the target/clutter kernels is obtained by

$$K(\xi_k, T) = e^{-\frac{d(\xi_k, t)}{\alpha}}; \quad K(\xi_k, C) = e^{-\frac{d(\xi_k, c)}{\alpha}} \qquad (2)$$

where $d(\xi_k, \xi)$ is the geodesic distance of $\mathbb{S}^2$ and α is a normalization parameter. Note that a position on the sphere ξ_k has a high value in the ordering function $h(\xi_k)$ when is located close to the target set and far from the set clutter. When dealing with multimodal clutter, the information from the various clutters has to be included. Thus, in $K(\xi_k, C)$ the contributions of all the different clutters should be combined. The mapping has to be balanced, i.e., for monomodal target training set, its weight has to be as significant as the combination of the clutters. Otherwise, points belonging to T are drawn to the clutter and its values in the ordering function are erroneously decreased. Let us assume P different clutters, characterized by their corresponding Fréchet means on the sphere: $C_1 = \mathcal{V}_\bot^1 = \{c_j\}_{j=1}^{J_1} \to c_1 = \mu^\circ(C_1); C_2 = \mathcal{V}_\bot^2 = \{c_j\}_{j=1}^{J_2} \to c_2 = \mu^\circ(C_2); \cdots C_P = \mathcal{V}_\bot^P = \{c_j\}_{j=1}^{J_P} \to c_P = \mu^\circ(C_P)$. The proposed formulations for computing the kernels are detailed below.

Combination by addition. Having identified all clutter training sets and characterized them by their Fréchet mean $c_i = \mu^\circ(C_i)$. The kernel for each set is computed individually, then, for the whole clutter, the values from all the kernels are added up, i.e.,

$$K(\xi_k, C) = \sum_{p=1}^P K(\xi_k, C_p) = \sum_{p=1}^P e^{-\frac{d(\xi_k, c_i)}{\alpha}} \qquad (3)$$

In order to keep the balance for the target training set, its corresponding kernel is weighted according to the number of clutter, i.e.,

$$K(\xi_k, T) = P \cdot K(\xi_k, \mathcal{V}_T) = P \cdot e^{-\frac{d(\xi_k, t)}{\alpha}} \qquad (4)$$

Combination by distance. For a given ξ_k, we compute the kernels for each training set C_i and we select the kernel with the largest value to describe the whole clutter set, i.e., such that $K(\xi_k, C_p) > K(\xi_k, C_p)$, $\forall q \neq p$. For the position ξ_k, the chosen clutter is the more restrictive and representative. Due to the fact that the clutter C_p is the closest set to ξ_k, i.e. at minimum distance. The kernel referred in Eq. (2) is used for the training target set.

Combination by grouping. We define a global clutter set which is the result of lumping together all C_i: $C = \{C_1 \cup C_2 \cup \cdots \cup C_P\} = \{c_j\}_{j=1}^M$, where $M = \sum_{p=1}^P J_p$. The Fréchet mean of the global set C has no geometrical sense anymore: as it is located at the barycenter of C, most of the points belonging to the different original clutter sets would be far from it, and so, it would not be significant. The distances

accumulated to each element of the set C and of the set T are computed instead as

$$K(\xi_k, C) = \sum_{j=1}^{M} \frac{1}{1 + d(\xi_k, c_j)}; K(\xi_k, T) = \sum_{i=1}^{I} \frac{1}{1 + d(\xi_k, t_i)} \quad (5)$$

Remark that it is necessary that $M = I$ for a balanced mapping function. When target is multimodal instead, the same considerations need to be done, as for both multimodal target and clutter.

4. MORPHOLOGICAL DETECTORS

We extend here, some of the morphological transformations using the h-orderings above developed. Let $f(x,y) \in \mathcal{F}(E, \mathbb{S}^2)$ be an image valued on the sphere. Given the partial ordering induced by h, denoted by $\leq_h$, the *supervised dilation on the sphere* and *supervised erosion on the sphere* of an image $f(x,y) \in \mathcal{F}(E, \mathcal{L})$ are obtained replacing the operators sup and inf for $\vee_h$ and $\wedge_h$ according to $\leq_h$, i.e.,

$$\delta_{h,B}(f)(x,y) = \{\vee_h [f(u,v)], (u,v) \in B(x,y)\} \quad (6)$$
$$\varepsilon_{h,B}(f)(x,y) = \{\wedge_h [f(u,v)], (u,v) \in \check{B}(x,y)\} \quad (7)$$

The supervised erosion $\varepsilon_{h,B}(f)$ typically contracts the structures of image f with a value on the sphere close to the training set T of foreground (usually associated to target to be detected). It also expands the regions close to the training set C of background (or clutter zones). Dually, the dilation performs an enlargement of the structures located near foreground and dwarfs the corresponding pre-defined background.

All the other morphological operators, defined as products of dilations and erosions are generalized to the supervised framework of $\mathbb{S}^2$.

4.1. Supervised hit-or-miss transformation in $\mathbb{S}^2$

In mathematical morphology, hit-or-miss transform (HMT) is an operation that detects a given configuration or pattern in a binary image, using the morphological erosion operator and a pair of disjoint structuring elements. The result of the hit-or-miss transform is the set of positions, where the first structuring element has to match in the foreground, while the second structuring element has to match the background. Let us denote $S_1 \subset E$, $S_2 \subset E$ the pair of SEs, where $S_1 \cap S_2 = 0$. Then we look for all the positions where S_1 fits within a binary image I and S_2 within its complement image I^c. That can be formulated in terms of the morphological erosion, i.e.,

$$HMT(I; S_1, S_2) = \varepsilon_{S_1}(I) \cap \varepsilon_{S_2}(I^c).$$

Let us generalize the hit-or-miss transformation to images valued on the sphere. It can be used to point out and to extract those structures on an image $f(x,y) \in \mathcal{F}(E, \mathbb{S}^2)$ with

a prior known shape and placed on a specific location on the sphere surface. For the HMT, the first structuring element has to match in the foreground. Once we have established the h-supervised ordering for the pair of sets $\{T, C\}$, the supervised erosion associated to S_1 is directly computed. Whereas matching the background, we induce an inverse ordering by interchanging the sets $\mathcal{V}_\top$ by $\mathcal{V}_\bot$, i.e., $\{T, C\}$ is treated as $\{C, T\}$. The hit-or-miss transform on the sphere can be written as

$$HMT(f; S_1, S_2)(x,y) = \varepsilon_{h_1, S_1}(f)(x,y) \wedge \varepsilon_{h_2, S_2}(f)(x,y) \quad (8)$$

where

$$h_1 = h\{T, C\}|h(b) = \bot, h(t) = \top\}$$
$$h_2 = h\{C, T\}|h(b) = \top, h(t) = \bot\}$$

Each structuring element S_i has a training set associated $\{S_1, T\}, \{S_2, C\}$. Thus, the formulation given in (8) can be generalized based on the sets of couples $\{S_i, B_i\}_{i=1,\cdots,I}$, with all the SEs S_i disjoint where the B_i represent the sets of values on the sphere associated. This approach is widely explained in [9]. However, we limit here our developments on the sphere to the HMT formulation for a single pair $\{T, C\}$ and a single pair of structuring elements for the target S_1 and for the clutter S_2. In the multimodal cases, the different sets are rather combined while defining the function h of ordering. We can also include a threshold ϵ to allow a degree of noise in the detection. This parameter needs to take the same value for both erosions, meaning the mapping that defines the ordering is balanced. More precisely, it is defined by

$$HMT_\epsilon(f; S_1, S_2)(x,y) = \quad (9)$$
$$(\varepsilon_{h_1, S_1}(f)(x,y) \wedge \varepsilon_{h_2, S_2}(f)(x,y)) < \epsilon$$

Fig. 2 depicts various examples of HMT_ϵ for different types of targets to be detected over different clutters.

(a) $f(x,y)$ (b) $HMT(f; S_1, S_2)(x,y)$ (c) $HMT(f; S_1', S_2')(x,y)$
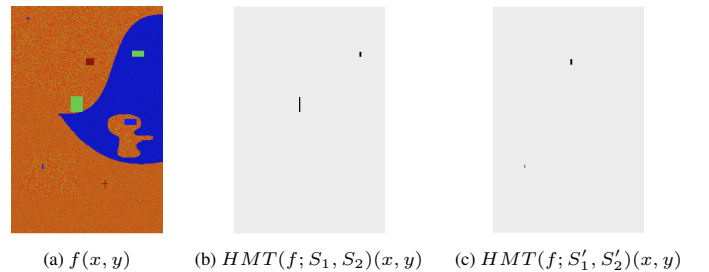
Fig. 2. (a) Original image, (b) monomodal target and multimodal clutter and (c) multimodal target and monomodal clutter.

4.2. Restricted supervised top-hat in $\mathbb{S}^2$

A natural extension for the *supervised opening on the sphere* is defined as a supervised erosion followed by a supervised

dilation:

$$\gamma_{h,B}(f)(x,y) = \delta_{h,B}\left(\varepsilon_{h,B}(f)(x,y)\right) \qquad (10)$$

Its corresponding *supervised positive top-hat on the sphere* is the residue between the original image and its supervised opening:

$$\rho_{h,B}^{+}(f)(x,y) = d(f(x,y),\gamma_{h,B}(f)(x,y)) \qquad (11)$$

with $d(\xi_i,\xi_j)$ the Riemannian distance on $\mathbb{S}^2$. Abrupt changes in the clutter and targets, smaller than the structuring element B and different from the ilk intended to detect, are removed when computing the opening and consequently appears in the top-hat. They introduce false positive detections, as illustrated in Fig. 3(b). A different methodology based on the decomposition of the sets in *h-supervised ordering* is proposed. Let T_i, $i = 1,\cdots,I$ the target sets found in the image and C_j, $j = 1,\cdots,J$ the corresponding clutter sets. Moreover, the type of target expected to be detected conforms the particular set T_m.

Fixing T_m, marginal orderings can be defined for each pair $\{T_m,C_j\}$, $\forall j$ and $\{T_m,T_i\}$ $\forall i \neq m$. According to the analysis given in Section 3, we can formulate the ordering mappings:

$$h_i(\xi_k) = K(\xi_k,T_m) - K(\xi_k,T_i) = e^{-\frac{d(\xi_k,t_m)}{\alpha}} - e^{-\frac{d(\xi_k,t_i)}{\alpha}}$$

$$h_j(\xi_k) = K(\xi_k,T_m) - K(\xi_k,C_j) = e^{-\frac{d(\xi_k,t_m)}{\alpha}} - e^{-\frac{d(\xi_k,c_j)}{\alpha}}$$

with $i = 1,\cdots,I$ but $i \neq m$ and $j = 1,\cdots,J$. Hence, we construct every supervised opening $\gamma_{h_l,B}(f)$ according to every marginal ordering h_l, $l = 1,\cdots,L$ (with $L = I + J - 1$). The difference between the original image and the supervised openings form the ensemble of marginal top-hats, $\rho_{h_l,B}^{+}(f)(x,y) = d(f(x,y),\gamma_{h_l,B}(x,y))$. Now, we can define the *restricted supervised top-hat on the sphere* with respect to target T_m as the pixelwise minimum of all the supervised top-hats $\{\rho_{h_l,B}^{+}\}_{l=1}^{L}$:

$$\rho_{T_m,B}^{+}(f)(x,y) = \min_{l=1,\cdots,L}\{\rho_{h_l,B}^{+}(f)(x,y)\} \qquad (12)$$

False positive detections can appear in some of the marginal supervised top-hats, its value may be even higher than the value required for a target. For a structure to be hold in the restricted supervised top-hat, it has to be present in all the marginal top-hats $\rho_{h_l,B}^{+}$, $\forall l$ with a significant value. By choosing the minimum, the target expected takes the lower value found, and detection resolution is deteriorated. On the other hand, undesired targets and clutter changes are dismissed as they are not present in all $\rho_{h_l,B}^{+}$, $\forall l$. Fig. 3(c) illustrates an example of the performance of restricted supervised top-hat, in comparison with the marginal ones.

5. CONCLUSIONS AND PERSPECTIVES

Supervised ordering methods proposed in this paper allow an extension formally correct of the mathematical morphology

(a) $f(x,y)$ (b) $\rho_{h,B}^{+}(f)(x,y)$ (c) $\rho_{T_m,B}^{+}(f)(x,y)$
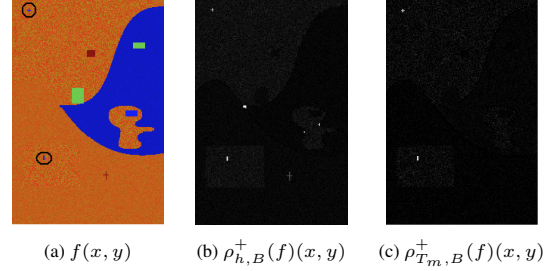
Fig. 3. (a) Original image, (b) positive top-hat with the h-supervised ordering and (c) restricted supervised top-hat. Abrupt changes in the clutter are enhanced and cross form object on the bottom right sight of the image does not correspond to the set desired targets T_m.

on images valued on $\mathbb{S}^2$. A prior knowledge about the kinds of values in the image is required. If this training set is available, the associated operators may be extremely accurate in the target detection.

Since in many practical applications prior information is limited, strategies capable to automatically determine targets/clutters in the image should be considered, for example clustering algorithms on the sphere (e.g. k-means) or statistical modeling of distributions (e.g. E-M algorithm).

6. REFERENCES

[1] P.T. Fletcher, S. Venkatasubramanian, S. Joshi. *Robust Statistics on Riemannian Manifolds via the Geometric Median*. In Proceedings of CVPR'08, 2008.

[2] S. Fiori. *On vector averaging over the unit hypersphere*. Digital Signal Processing, 19:715–725, 2009.

[3] A. Hanbury, J. Serra. *Morphological Operators on the Unit Circle*. IEEE Transactions on Image Processing, 10(12):1842–1850, 2001.

[4] J. Serra. *Image Analysis and Mathematical Morphology, Vol I*. Academic Press, NY, London, 1982.

[5] J. Serra. *Anamorphoses and Function Lattices (Multivalued Morphology)*. In (Dougherty, Ed.) Mathematical Morphology in Image Processing, Marcel-Dekker, 483–523, 1992.

[6] P. Soille. *Morphological Image Analysis*. Springer-Verlag, Berlin, 1999.

[7] S. Velasco-Forero, J. Angulo. *Supervised ordering in R^n: Application to morphological processing of hyperspectral images*. IEEE Transactions on Image Processing, 20(11): 3301–3308, 2011

[8] S. Velasco-Forero, J. Angulo. *Morphological processing of hyperspectral images using kriging-based supervised ordering*. In ICIP(2010) 1409-1412

[9] S. Velasco-Forero, J. Angulo. *Hit-or-Miss Transform in Multivariate Images*. In Proceedings of ACIVS (1)'2010. pp.452 463